Ab Initio Investigation of a Possible Liquid-Liquid Phase Transition in $MgSiO_3$ at Megabar Pressures

Burkhard Militzer

Department of Earth and Planetary Science, Department of Astronomy, University of California, Berkeley, CA 94720, USA

Abstract

We perform density functional molecular dynamics simulations of liquid and solid $MgSiO_3$ in the pressure range of 120−1600 GPa and for temperatures up to 20000 K in order to provide new insight into the nature of the liquid-liquid phase transition that was recently predicted on the basis of decaying laser shock wave experiments [Phys. Rev. Lett. 108 (2012) 065701]. However, our simulations did not show any signature of a phase transition in the liquid phase. We derive the equation of state for the liquid and solid phases and compute the shock Hugoniot curves. We discuss different thermodynamic functions and by explore alternative interpretations of the experimental findings.

Keywords: density functional molecular dynamics, ab initio simulations, high pressure, shock wave experiments

1. Introduction

The recent work by D. K. Spaulding *et al.* [1] reported results from decaying laser shock wave experiments which provided evidence of a liquid-liquid phase transition in $MgSiO_3$ at megabar pressures. The authors measured a reversal in the shock velocity and thermal emission and interpreted their findings in terms of a liquid-liquid phase transition that occurs when the sample changes from a high density to a low density fluid state during shock decay. Decaying shock experiments are a new experimental technique that allows one to map out a whole segment of the Hugoniot curve with a single shock wave experiment.

First-principles computer simulations have a long tradition of characterizing materials at extreme pressures [2, 3, 4] and temperatures [5, 6, 7] and of contributing to the interpretation of shock wave experiments [8, 9, 10]. The goal of this particular paper is to perform density functional molecular dynamics simulations (DFT-MD) of dense liquids [8] in order to verify the predictions of a liquid-liquid phase transition by Spaulding *et al.* [1]. First order transitions in liquids are unusual but have been seen in experiments on phosphorus and in simulations of dense hydrogen [11].

2. Simulation Parameters

All simulations were performed with the VASP code [12] with pseudopotentials of the projector-augmented wave type [13], a cut-off for the expansion of the plane wave basis set for the wave functions of 500 eV, and the PBE exchange-correlation functional [14]. The Brillioun zone was only sampled with the Γ point to allow for extended and efficient MD simulations. Our simulations lasted between 1 and 20 ps and used a small time step of 0.2 fs. The electronic states were populated according to the Mermin functional [15].

We used an orthorhombic supercell with 60 atoms that we constructed by tripling the unit cell of the post-perovskite (PPV) structure that we relaxed at 120 GPa. The system was heated and melted using a Nosé thermostat. We then explored the liquid state by scaling the velocities and changing the density accordingly.

We also performed heat-until-it-melts simulations with 60 atoms starting a perfect PPV crystal at hydrostatic conditions. We then gradually increased the temperature in a fixed cell geometry. We also performed a large number of solid simulations at constant temperature and different densities.

3. Results and Discussion

The P-T conditions of our simulations are shown in Fig. 1 and the resulting equation of state (EOS) for the liquid and the post-perovskite solid phases are given in Tables 1 and 2. Initially we focused our work on 7500 K and 12500 K in order to maximize the likelihood of directly observing a phase transition in the liquid during the MD simulations. However, all the thermodynamic functions, that we analyzed, varied in a perfectly smooth way as function of temperature and pressure. Figure 2 shows the volume and the internal energy as function of pressure. The zero of energy was set equal to

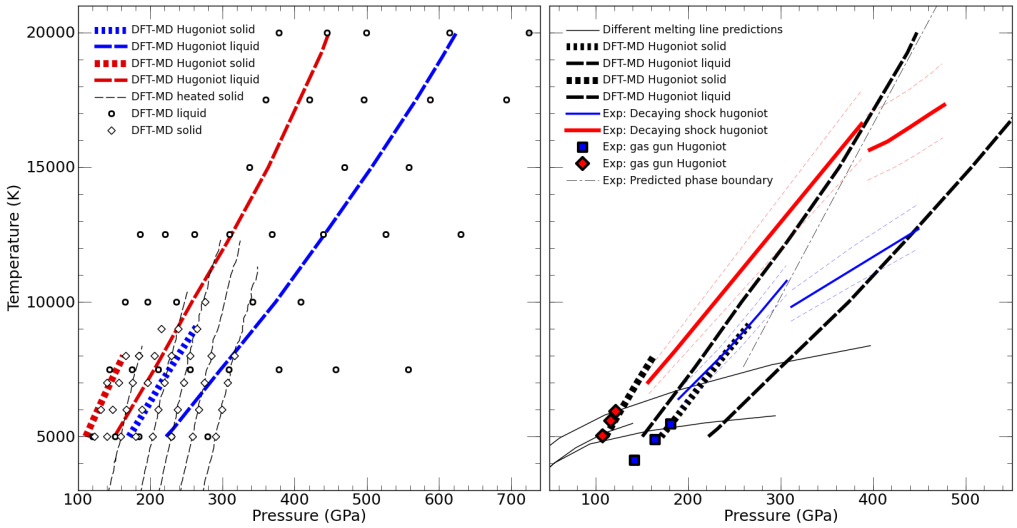

Figure 1: In the left diagram, the open diamond and circles indicate the pressure-temperature conditions of our solid and liquid $MgSiO_3$ DFT-MD simulations, respectively. The thin black dashed lines show the P-T paths of the solid portions of our heat-until-it-melts simulations. The computed solid and liquid shock Hugoniot curves are shown in blue and red color corresponding to initial densities of 3.22 and 2.74 $\mathrm{g\,cm^{-3}}$ to match those of the single crystal (blue) and glass (red) materials used in the experiments [1]. The Hugoniot curves are repeated in black and white on the right for comparison with the decaying shock measurements [1]. From the discontinuities in the experimental Hugoniot curves, the phase boundary between a high and low density liquid was inferred (dash-dotted line). The computed Hugoniot curve for solid $MgSiO_3$ agree well with earlier gas gun shock measurements (diamonds) [16, 17]. Three earlier predictions of the melting line are included [18, 19, 20].

the energy of a collection of isolated atoms. We conclude from this analysis, if there exists a phase transition in the liquid phase then *ab initio* simulations of 60 atoms are unlikely to spontaneously transform into a different phase.

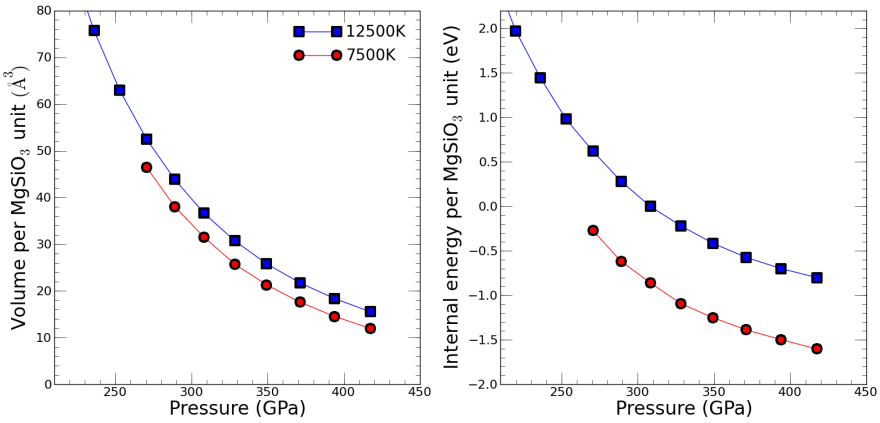

Figure 2: Volume and internal energy as function of pressure derived from DFT-MD simulations of liquid $MgSiO_3$. Both functions are smooth and exhibit no indication of a phase transition.

We computed the shock Hugoniot curve from the usual relation [21],

$$H = E - E_0 + \frac{1}{2}(V - V_0)(P + P_0) = 0, \tag{1}$$

where the initial volume, V_0=51.77 Å^3, and initial internal energy, $E_0 = -35.914$ eV per $MgSiO_3$ formula unit (FU), were taken from a DFT calculation of enstatite at 3.22 g cm^{-3} that we performed. We used the same E_0 to derive the Hugoniot curves for a glass sample with an initial density of 2.74 g cm^{-3}. P_0 was assumed to be zero because $P_0 \ll P$ is satisfied for all final states.

The resulting DFT-MD Hugoniot curves for liquid and crystalline $MgSiO_3$ are shown in Fig. 1. Our results for the solid phase agree well with the earlier shock measurements using a gas gun [16, 17]. However, the agreement with the decaying laser shock results is not satisfactory. A portion of our computed Hugoniot curve for the solid at $\rho_0 = 3.22$ g cm^{-3} overlaps with the measurements in the temperature range from 7000 to 9000 K. Also at 450

$T(K)$	time (ps)	ρ (g cm^{-3})	P (GPa)	E/FU (eV)
5000	1.47	4.7921	120.0(5)	−23.98(7)
5000	1.31	5.0796	151.5(8)	−22.75(9)
5000	1.34	5.3905	184.3(9)	−21.91(8)
5000	5.02	5.7273	228.8(5)	−20.10(4)
5000	5.43	6.0928	279.3(5)	−17.99(2)
7500	4.90	4.7921	143.4(5)	−19.23(7)
7500	4.99	5.0796	174.5(5)	−17.97(9)
7500	4.93	5.3905	211.2(4)	−16.66(8)
7500	4.66	5.7273	255.4(5)	−15.01(8)
7500	4.67	6.0928	308.9(7)	−13.12(9)
7500	5.94	6.4900	377.9(6)	−10.31(7)
7500	5.60	6.9225	456.6(8)	−7.40(9)
7500	5.78	7.3944	557.4(7)	−3.26(9)
10000	1.17	4.7921	165.0(8)	−14.41(12)
10000	1.24	5.0796	196.6(1.1)	−13.24(19)
10000	1.14	5.3905	236.5(9)	−11.94(11)
10000	4.94	6.0928	341.3(7)	−7.63(6)
10000	5.30	6.4900	408.6(9)	−5.10(13)
12500	22.94	4.7921	186.2(3)	−9.61(4)
12500	17.24	5.0796	220.3(4)	−8.38(6)
12500	12.72	5.3905	260.8(3)	−6.88(7)
12500	17.99	5.7273	309.5(3)	−4.98(5)
12500	15.74	6.0928	368.7(3)	−2.63(6)
12500	3.52	6.4900	439.4(1.0)	−0.01(13)
12500	3.63	6.9225	526.4(1.2)	3.39(18)
12500	4.36	7.3944	629.7(1.0)	7.44(14)
12500	4.77	7.9101	755.2(8)	11.78(6)
12500	4.72	8.4749	908.8(1.2)	17.36(17)
12500	4.80	9.0948	1094.4(1.8)	23.66(17)
12500	5.02	9.7766	1326.5(1.7)	31.8(2)
12500	18.83	10.5283	1604.8(1.1)	41.18(14)
15000	3.34	5.7273	337.0(1.0)	0.11(16)
15000	3.75	6.4900	468.9(8)	5.01(10)
15000	3.88	6.9225	558.4(1.1)	8.56(14)
17500	1.49	5.7273	359.9(1.7)	4.48(20)
17500	3.30	6.0928	420.6(8)	6.64(11)
17500	2.18	6.4900	495.9(1.0)	9.78(14)
17500	3.65	6.9225	587.5(1.1)	13.42(13)
17500	3.69	7.3944	692.8(1.1)	16.96(14)
20000	1.41	5.7273	377.6(1.4)	8.3(2)
20000	2.70	6.0928	444.3(6)	11.10(11)
20000	4.62	6.4900	499.4(6)	9.21(11)
20000	3.38	6.9225	614.1(1.2)	17.96(18)
20000	3.56	7.3944	724.5(1.0)	22.06(14)

Table 1: Temperature, MD simulation time, density, pressure and internal energy from our DFT−MD simulations of liquid $MgSiO_3$. The 1σ uncertainties of the trailing digits are given in brackets.

$T(K)$	time (ps)	ρ (g cm^{-3})	P (GPa)	E/FU (eV)
5000	4.23	5.0796	122.86(16)	−26.135(11)
5000	4.33	5.2320	139.94(19)	−25.591(12)
5000	4.59	5.3905	158.71(10)	−24.927(5)
5000	3.85	5.5555	179.59(14)	−24.196(9)
5000	5.00	5.7273	203.19(16)	−23.339(9)
5000	4.74	5.9063	229.46(12)	−22.380(8)
5000	5.00	6.0928	258.19(18)	−21.293(5)
5000	5.00	6.2872	290.29(14)	−20.068(7)
6000	4.18	5.0796	131.24(15)	−24.737(13)
6000	4.29	5.2320	147.89(14)	−24.217(7)
6000	4.50	5.3905	166.75(17)	−23.584(9)
6000	3.83	5.5555	188.2(2)	−22.825(14)
6000	4.75	5.7273	211.29(14)	−21.998(8)
6000	4.73	5.9063	237.50(15)	−21.049(8)
6000	5.00	6.0928	266.9(2)	−19.979(6)
6000	5.00	6.2872	299.11(14)	−18.748(5)
7000	4.11	5.0796	139.7(2)	−23.25(3)
7000	4.92	5.2320	156.41(12)	−22.768(17)
7000	4.86	5.3905	175.31(15)	−22.170(14)
7000	3.81	5.5555	196.05(13)	−21.410(17)
7000	4.73	5.7273	219.72(14)	−20.632(10)
7000	4.64	5.9063	246.1(2)	−19.672(9)
7000	5.00	6.0928	274.90(12)	−18.611(7)
7000	5.00	6.2872	307.1(2)	−17.397(12)
8000	4.87	5.2320	165.6(2)	−21.17(3)
8000	4.39	5.3905	184.5(3)	−20.58(4)
8000	4.39	5.3905	184.5(3)	−20.58(4)
8000	3.75	5.5555	205.8(3)	−19.90(3)
8000	5.00	5.7273	229.08(20)	−19.122(18)
8000	4.62	5.9063	255.10(19)	−18.204(15)
8000	5.00	6.0928	284.2(2)	−17.163(17)
8000	5.00	6.2872	316.3(2)	−15.964(12)
9000	3.62	5.5555	215.1(3)	−18.27(2)
9000	5.00	5.7273	238.9(3)	−17.50(2)
9000	4.26	5.9063	264.4(3)	−16.63(2)
10000	4.53	5.9063	275.6(3)	−14.84(3)

Table 2: Temperature, MD simulation time, density, pressure and internal energy from our DFT-MD simulations of crystalline post-perovskite $MgSiO_3$. The 1σ uncertainties of the trailing digits are given in brackets.

GPa and 12500 K, the calculated Hugoniot curve for the liquid agrees with the measurements but the slope of the theoretical Hugoniot curve is different and it shows no sign of a phase transition. The agreement for an initial density of 2.74 $\mathrm{g\,cm^{-3}}$ is again not favorable. The theoretical Hugoniot the liquid passes right through the T-P conditions where a phase transformation is predicted based on the experimental data but DFT-MD simulations do not exhibit one.

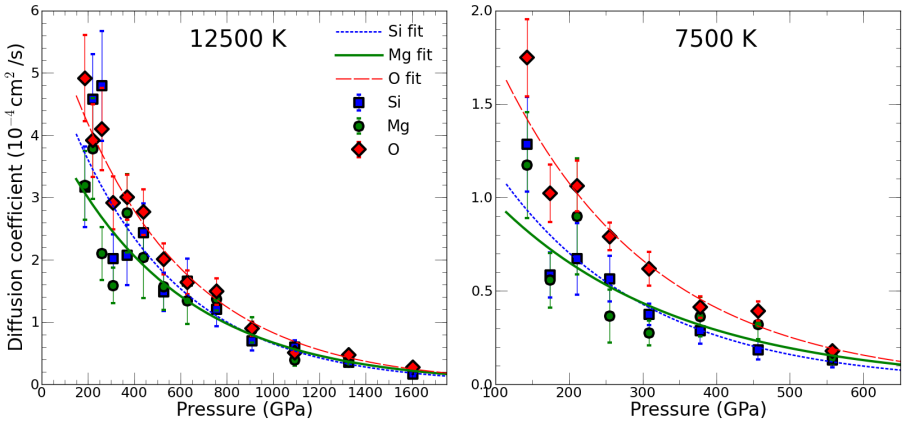

Figure 3: Diffusion coefficients of Mg, Si, and O ions as function of pressure for 7500 and 12500 K inferred from DFT-MD simulations. The lines show fits to an exponential function of pressure for each species.

Next we investigated the possibility of the existence of a superionic phase between the solid and the liquid phases where some ions remain stationary while others diffuse throughout the material like in a liquid [22]. In Fig. 3, we plot the diffusion coefficients as a function of pressure. At 12500 K, all ions diffuse at the same rate approximately. At 7500 K, the diffusion is slower as one would expect in the fluid near the melting line. The oxygen ions diffuse a bit faster than the magnesium and silicon ions but there is no evidence for a superionic state.

We also performed heat-until-it-melts simulations of solid samples (Fig. 1) that we isochorically heated at a rate of 1000 K per picosecond. This approach was used to predict the superionic state of water [22] but our sample always went into a fully fluid state after a substantial amount of superheating. Figure 4 shows that the liquid always exhibits a higher pressure than the

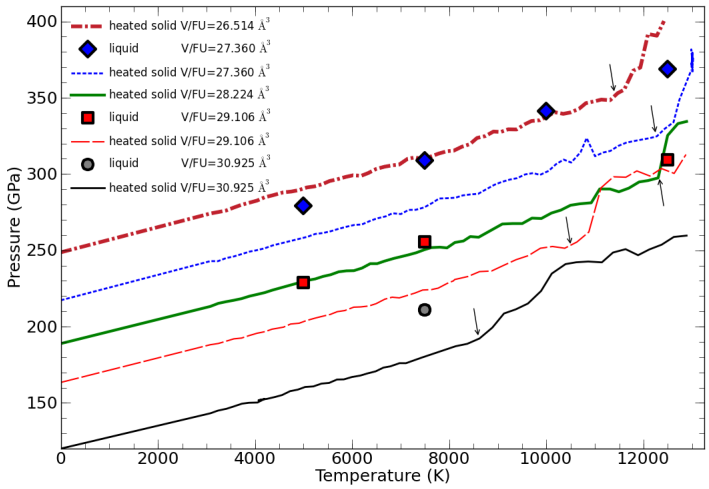

Figure 4: The pressure-temperature behavior during heat-until-it-melts simulations (lines) is compared with isothermal liquid simulations (symbols). The small arrows indicate the beginning of the melting transformation in the MD simulation. Liquid samples are found to always exhibit a higher pressure than solid ones at the same density.

solid when compared for the same density and temperature. This means, for given temperature and pressure, the solid is always denser than the liquid. Therefore the melting line of PPV $MgSiO_3$ is expected to have a positive Clapeyron slope [23].

We performed our simulations with only 60 atoms and all results may need to be confirmed with larger simulations that possibly also use more k-points. Our longest simulations ran for 20 ps, which is fairly long for *ab initio* calculations. If a new liquid phase emerges, one would expect to observe a spontaneous phase transformation, as long as it does not involve any large-scale rearrangements of atoms. If liquid $MgSiO_3$ phase-separates into a MgO-dominated and a SiO_2-rich fluid, as was predicted for the solid at approximately 1000 GPa [24], we would most likely not be able to observe this process in our simulations. One would instead need to perform more expensive Gibbs free energy calculations [25, 26, 4, 27, 28] but such a complex effort goes beyond this investigation.

Furthermore, if there existed a new, unknown phase in the $MgSiO_3$ phase diagram, it does not have to be a liquid. One could imagine a new stable

solid phase that introduces a solid-solid-liquid triple point and may lead to an increase in the slope of the melting line. At zero temperature, existence of a post-post-perovskite phase has been intensely studied with *ab initio* random structure search algorithms and no such phase has been found but a new, entropy-stabilized phase may still exist at high temperature. In principle, this solid-solid-liquid triple point could also be between perovskite (PV), PPV, and liquid phases. This point has not yet been determined neither with experimental nor with theoretical means but PV-to-PPV transition pressure is known to increases with temperature.

One may also ask whether there exists an alternative interpretation for the experimental observations. Our first recommendation would be to repeat those measurements with steady shock wave experiments in order to verify the discontinuities on the principal Hugoniot curve of $MgSiO_3$. This may require a series of shock experiments with relatively small error bars but it would be an important confirmation.

It is also possible that observed shock velocity reversal is related to the melting transition of $MgSiO_3$. Figure 1 shows that most of the experimental results fall in between the computed Hugoniot curves for the solid and the liquid. However, the temperatures are too high for a solid phase to be thermodynamically stable. Phase transition temperatures of 10 000 and 16 000 K have been predicted based on the measurements of single-crystal and glass material [1], respectively. Nevertheless it is interesting to discuss the behavior of decaying shock experiments in the presence of a melting transition. Some material behind the shock front may freeze during the shock decay. This could introduce a secondary wave and thereby affect the behavior of the shock front.

At the beginning of a decaying shock experiments, the sample material is compressed to a state of high pressure and high temperature on the principal Hugoniot curve. As the shock decays, new material does not reach as high pressures and temperatures but stays on the Hugoniot curve, which allows one to map out the whole Hugoniot curve with just one shock measurement. The question is what happens to the material that had compressed to a higher P-T state earlier. One may assume that the whole region behind the shock front will equilibrate to a new pressure, which we labeled P^* in Fig 5. Any parcel of material that was shocked to a high P-T state will adiabatically expand [21] to reach P^* and slow down to travel at the new and reduced particle velocity. Since this expansion is gradual and not associated with any shock, one typically also assumes that this expansion is isentropic [21]

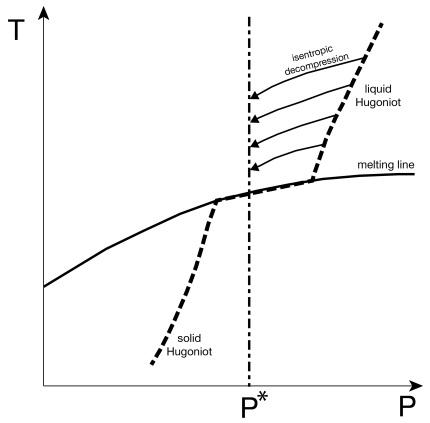

Figure 5: Temperature-pressure diagram with melting lines and shock Hugoniot curves. The arrows indicate the adiabatic and isentropic expansion of material during decaying shocks. The graph shows a material with normal melting behavior with a positive Clapeyron slope, $dT_m/dP > 0$.

(arrows in Fig. 5). While one assumes a new pressure, P^*, is established, the entire sample behind the shock front is not expected to reach thermal equilibrium during the experiment. This leads to the situation where hot material at a lower density is pushing on colder material at a higher density. This could lead to a fluid dynamic instability of Rayleigh-Taylor type if the density contrast becomes too high and the time scale is long enough for such an instability to develop.

It is important to note that Hugoniot curves are steeper in P-T space than isentropes, $\frac{\partial T}{\partial P}\big|_{\rm Hug} > \frac{\partial T}{\partial P}\big|_S$. The shock front on the Hugoniot curve would always enter any new thermodynamic phase, that may exist at lower temperature, before the hotter material behind the shock front reaches it.

However, the melting transition may have an effect on the shock propagation at much higher temperature. Zeldovich and Raizer [21] showed that a shock will split into two waves if the shock Hugoniot curves intersects with the Rayleigh line that linearly connects the initial and final states in a P-V diagram. If the melting transition would introduce such a splitting, it would affect the shock propagation at much higher temperatures and pressures. We plotted our liquid and solid Hugoniot curves the P-V and u_s-u_p diagrams in Figures 6 and 7. For each of the Hugoniot curves, let us assume that ma-

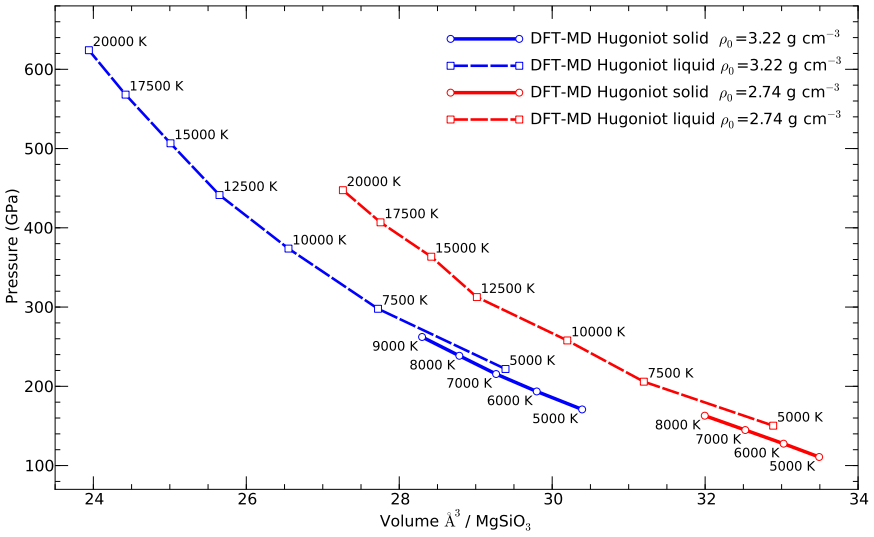

Figure 6: P-V diagram of the solid and liquid segments of the shock Hugoniot curves for two initial densities. The labels indicate the calculated shock temperatures.

terial melts at a temperature, T_m, somewhere in the range spanned by the calculation in Refs. [18, 19, 20] (see Fig. 1). If there occurred a sudden and complete phase change from liquid to solid during a decaying shock experiments at T_m, it would lead to a abrupt drop in pressure, density, shock and particle velocities because intermediate values cannot be realized by either phase while satisfying Eq. (1).

From Fig. 6, we conclude that the Hugoniot curves do not intersect with the Rayleigh line but the material must assume a mixed state because the particle velocity decreases gradually in a decaying shock wave experiment. Following the arguments that Greeff *et al.* [29] applied to the α-to-ω transition in solid titanium, the properties of a solid-liquid $MgSiO_3$ mixture with the solid fraction, λ, can be derived from

$$E = (1-\lambda)E_l(P,T) + \lambda E_s(P,T) \quad (2)$$

$$V = (1-\lambda)V_l(P,T) + \lambda V_s(P,T) \quad (3)$$

for a given pair of T and P on the melting line. Under the assumption of thermodynamic equilibrium, λ can derived from Eq. (1) for given pressure

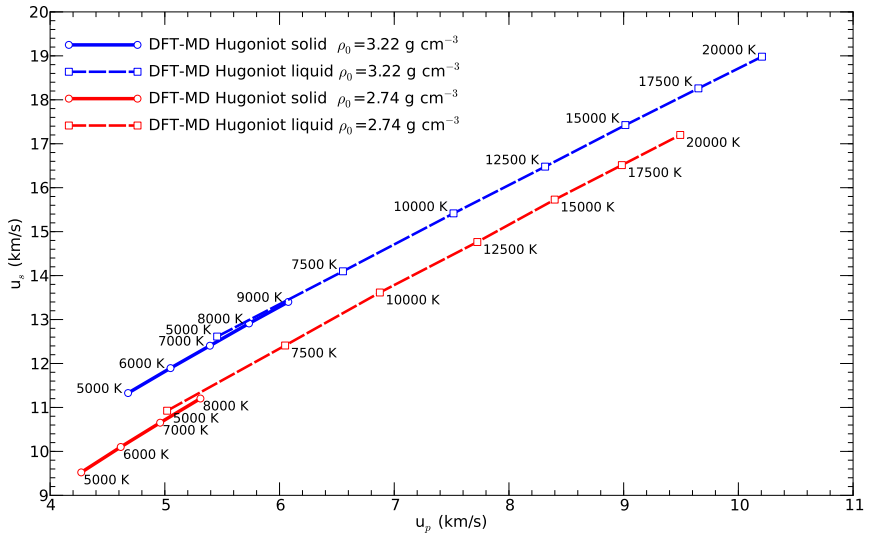

Figure 7: Shock velocity versus particle velocity for the Hugoniot curves from Fig. 6.

or particle velocity. For high shock velocities, the final state of the material is fully molten. As the shock decays, the solid fraction gradually increases until the shock is too weak to introduce any melting.

We now want to address the question what happens as the parcels of solid-liquid mixtures expand adiabatically. The solid fraction, λ, must change to keep the entropy of the mixture,

$$S \;=\; (1-\lambda)S_l(P,T) + \lambda S_s(P,T) \;\;, \tag{4}$$

constant as the pressure decreases. T adjusts to the melting temperature for given pressure. If the solid fraction, λ, gradually increases during the expansion, the particle velocity directly behind the shock front would decrease. This is not unusual but the opposite case is much more interesting. If the liquid fraction increases during the shock decay, $\frac{\partial \lambda}{\partial P}\big|_{T_m} > 0$, it would imply an increase in particle velocity. As a result the shock wave would split in two waves, which would make the analysis of the VISAR signals much more difficult.

We can determine the thermodynamic parameters for such a shock wave splitting. During the expansion, the total entropy stays constant, $\frac{\partial S}{\partial P}\big|_{T_m} = 0$.

Eq. (4) implies,

$$\left.\frac{\partial \lambda}{\partial P}\right|_{T_m} (S_l - S_s) = (1-\lambda) \left.\frac{\partial S_l}{\partial P}\right|_{T_m} + \lambda \left.\frac{\partial S_s}{\partial P}\right|_{T_m} \tag{5}$$

Since the entropy of the liquid is always greater than that of the solid, a positive right term in Eq. (5) would imply that the shock wave splits into two separate waves as the decay shock experiment enter the regime of solid-liquid coexistence. Without a detailed calculations of the entropies in both phases, it is not possible to determine whether this occurs in $MgSiO_3$ because the Clapeyron slope enters into the calculation. However, the entropy is accessible with thermodynamic integration techniques and equation of state models [20]. So our hypothesis of shock wave splitting can be tested with experimental and theoretical techniques.

Summarizing we can say that whether a Rayleigh-Taylor instability exists, a new solid phase appears, the shock wave splits into two waves, or indeed a liquid-liquid phase transition is the reason for the observed shock velocity reversal remains to be determined with future experiments. Concluding our theoretical investigation, we can report that our DFT-MD simulations to not support the hypothesis of a liquid-liquid phase transition in $MgSiO_3$. We were not able to give an obvious alternative interpretation of the experimental findings but we do, however, suggest the measurements be repeated with steady shock waves. The experimental findings are very interesting nevertheless and will lead to a better understanding of magnesiosilicates at high temperature.

Acknowledgments

The work was supported by NSF and NASA. We thank D. K. Spaulding and R. Jeanloz for disucssions and comments on this manuscript.

References

[1] D. K. Spaulding *et al.*, Phys. Rev. Lett. 108 (2012) 065701.

[2] B. Militzer, W. H. Hubbard, J. Vorberger, I. Tamblyn, S. A. Bonev, Astrophys. J. Lett. 688 (2008) L45.

[3] S. A. Khairallah, B. Militzer, Phys. Rev. Lett. 101 (2008) 106407.

[4] H. F. Wilson, B. Militzer, Phys. Rev. Lett. 104 (2010) 121101.

[5] B. Militzer, W. Magro, D. Ceperley, Contr. Plasma Physics 39 1-2 (1999) 152.

[6] S. X. Hu, B. Militzer, V. N. Goncharov, S. Skupsky, Phys. Rev. Lett. 104 (2010) 235003.

[7] S. X. Hu, B. Militzer, V. N. Goncharov, S. Skupsky, Phys. Rev. B 84 (2011) 224109.

[8] B. Militzer, F. Gygi, G. Galli, Phys. Rev. Lett. 91 (2003) 265503.

[9] B. Militzer, Phys. Rev. Lett. 97 (2006) 175501.

[10] B. Militzer, Phys. Rev. B 79 (2009) 155105.

[11] M. A. Morales, C. Pierleoni, E. Schwegler, D. M. Ceperley, Proc. Nat. Acad. Sci. 107 (2010) 12799.

[12] G. Kresse, J. Furthmüller, Phys. Rev. B 54 (1996) 11169.

[13] P. E. Blöchl, Phys. Rev. B 50 (1994) 17953.

[14] J. P. Perdew, K. Burke, M. Ernzerhof, Phys. Rev. Lett. 77 (1996) 3865.

[15] N. D. Mermin, Phys. Rev. 137 (1965) A1441.

[16] J. A. Akins, S.-N. Luo, P. D. Asimow, T. J. Ahrens, Geophys. Res. Lett. 31 (2004).

[17] S.-N. Luo, J. A. Akins, T. J. Ahrens, P. D. Asimow, J. Geophys. Res. 109 (2004).

[18] N. de Koker, L. Stixrude, Geophys. J. Int. 178 (2009) 162.

[19] G. Shen, P. Lazor, J. Geophys. Res. 100 (1995) 17699.

[20] A. Zerr, R. Boehler, Science 262 (1993) 553.

[21] Y. B. Zeldovich, Y. P. Raizer, Elements of Gasdynamics and the Classical Theory of Shock Waves, Academic Press, New York, 1968.

[22] C. Cavazzoni, G. L. Chiarotti, S. Scandolo, E. Tosatti, M. Bernasconi, M. Parrinello, Nature 283 (1999) 44.

[23] S. Tateno, K. Hirose, N. Sata, Y. Ohishi, Earth Planet. Sci. Lett. 277 (2009) 130.

[24] K. Umemoto, R. M. Wentzcovitch, P. B. Allen, Science 311 (2006) 983.

[25] D. Alfè, M. J. Gillan, G. D. Price, Nature 405 (2000) 172.

[26] M. Morales *et al.*, Proc. Nat. Acad. Sci. 106 (2009) 1324.

[27] H. F. Wilson, B. Militzer, Astrophys. J 745 (2012) 54.

[28] H. F. Wilson, B. Militzer, Phys. Rev. Lett. 108 (2012) 111101.

[29] C. W. Greeff, D. R. Trinkle, R. C. Albers, J. Appl. Phys. 90 (2001) 2221.